ISSN: 2634 - 8853

Journal of Engineering and Applied Sciences Technology

SCIENTIFIC Research and Community

Research Article

Open Access

Experimental and Numerical Investigation of Phase Separation with Entrance Mixing

Weiwei E*, Kevin Pope and Xili Duan

Faculty of Engineering and Applied Science Memorial University of Newfoundland 230 Elizabeth Ave, St. John's, NL A1C 5S7, Canada

ABSTRACT

In this paper, experimental and numerical methods are used to investigate the separation of an oil / water mixture. An American Petroleum Institute (API) gravity-based separator was built to conduct the experimental studies. The numerical simulations were developed with the same geometry as the experimental setup. The effect of inlet velocity and the oil volume fraction on the separation process is investigated with the new numerical predictions. Validations of the simulation model show that the numerical predictions of the multiphase Volume of Fluid (VOF) model with the laminar viscosity model agree well with the experimental results. The results of oil volume fraction and velocity vector distribution in the separator showed that there was a mixing zone located at the entrance, which had a lower relative oil volume fraction and a higher velocity. The study of the inlet velocity effect on the mixing length of the entrance mixing zone shows that when the fluid in the separator is in the laminar range, the mixing length is less than 40% of the total separator length. However, when the inlet velocity was increased until the fluid in the separator reached the transient range, the mixing length occupied 90% of the total separator length.

***Corresponding author**

Weiwei E, Faculty of Engineering and Applied Science Memorial University of Newfoundland 230 Elizabeth Ave, St. John's, NL A1C 5S7, Canada; E-mail: ew3087@mun.ca

Received: May 26, 2021; **Accepted:** June 01, 2021; **Published:** June 04, 2021

Introduction

Separation of multiphase fluid systems is a common physical process in a wide variety of applications, including chemical and petroleum industries [1-4]. The most common form of a multiphase separator is a vertical or horizontal tank that has the function of providing sufficient residence time for the light phase to coalesce and separate from the heavier phase [5]. Gravity based separation utilizes the difference in specific gravities of the phases for separation, and the separation efficiency is affected by the density difference of these phases. As oil fields mature, the amount of produced water increases; therefore, separators need high efficiency for a variety of operating conditions. One method to improve efficiency is to improve coalescence. Rowley and Davies proposed a sedimentation-oriented model to better represent oil droplets between parallel plates, which enabled the smallest oil droplets to coalesce faster in a gravity separator, therefore improving the separation efficiency [6]. Aymong designed a separator with coalescence plates and diffusion blades to separate the oil-water-sand flow [7]. The function of these two structures was mainly to reduce the velocity and turbulence of the inlet flow, to provide more time for oil droplet coalescence around the plates' surfaces, and to increase oil and water separation efficiency.

Another method for improving separation efficiency is to extend the oil droplets' resident time. There are several ways to achieve this goal, such as adding inner components [8]. Lars Schlieper et al. investigated the required separator length with and without internals [9]. The experimental results stated that a maximum reduction of separation length up to 75% was achieved by adding inner plates. Therefore, they claim that a separator with internal components, such as plates, can be an appropriate aid for separator design due to their function of improving separation efficiency by reducing the turbulence of the inlet flow in the separator.

Computational fluid dynamics (CFD) applied to multiphase flow plays an essential role in modeling the oil / water separation process and for designing separators [10,11]. Table 1 presents a summary of the CFD simulation studies on operating conditions in a horizontal separator. Both two-dimensional (2-D) and three-dimensional (3-D) simulations are used in simulation studies. As presented in Table 1, CFD studies focus on three-phase and two-phase flows [12-21]. CFD simulations typically investigate the effect of operating pressure, flow rate, and fluid volume fraction on the separation efficiency. Also, some of the CFD studies investigate the separation of oil / water with different simulation models. The turbulence $k-\varepsilon$ model is one of the most popular models used to simulate multiphase separation [13,15,17,22]. For example, by using the Standard $k-\varepsilon$ model combined with the multiphase mixing model, Yuling et al. investigated the internal flow field inside a gravity separator focused on the effects of different components on internal flow fields [23]. They analyzed the velocity vector and flow field of two different inlet configurations and four different rectifiers. The simulation results showed that a separator with interval structures has better separation performance.

ANSYS Fluent provides three different models to simulate multiphase flow, which are the Mixture model, the VOF model, and the Euler-Euler model. Each of them is developed for different multiphase situations [24,25]. As shown in Table 1, the Euler-Euler model is the most popular model for simulating oil-water

multiphase flow [19,22]. Noroozi et al. used the Euler- Euler model to study the effect of different inlet designs on oil-water separation efficiency [26]. Four different inlet structures were simulated in the study: (1) an involute inlet structure with an angle of 20 ° relative to the horizontal coordinate, (2) an involute inlet design with a development curve ending, (3) an inlet orifice with an angle of 75 ° relative to the hydrocyclone axis, and (4) a partially static screw placed at the end of the inlet. Pressure distribution, velocity vector, and separation efficiency were measured and compared across these four structures. The study showed that using a helical inlet improved the separation efficiency by approximately 10%.

Table 1: Previous numerical research on gravity separation of multiphase systems

Authors	Modeling dimensions	Phases	pressure (kPa)	Flow velocity	rate/ Volume fraction	Temperature °C	Residence time (second)	Multiphase model	Note
Lee J. et al. 2009 [12]	3 D	Gas, oil, water	100, 400	Water: 117.25 m^3/h 690.27 Oil: m3/h	Oil: 85.5% Water: 14.5%	42, 50	240, 330	----	
Lee C. et al. 2004 [13]	3D	Gas, oil, water	690	Water: 491.87m^3/h Oil: 145.74 m3/h	Oil: 22.85% Water: 77.15%	50	15	----	Internal design study: Plate locations
Lu Y. et al. 2007 [14]	2D	Gas, oil, water	1280	Water: 631m3/h Oil: 435 m3/h	Oil: 40.81% Water: 59.19%	135	1130	----	With or without baffles
Austrheim T. 2006 [15]	3D	Gas, oil, water	2000, 5000, 9200	Water: 0.05-1.0 m3/h Oil: 0.05-1.0 m3/h	Oil: 0.2% Water: 0.2%	21	----	----	CFD & Experimental
Laleh P. 2010 [16]	3D	Gas, oil, water	70, 700, 2760	4 m/s	Oil: 27.3% Water: 72.7%	55.4	100	VOF+DPM k−ε	
Liang Y. et al. 2013 [17]	3D	Gas, oil, water	300	16, 18, 20, 22, 24 m3/h	Water: 64, 72, 80, 88, 96%	48	----	VOF+RNG k−ε	
Zhang X. et al. 2013 [18]	3 D	oil, water	1, 2, 5, 10	---	Oil: 95% Water: 5%	default	---		
Behin J. et al. [19] 2012	3 D	Gas, water	atmosphere	5, 7.5, 10 m3/h	Oil: 80% Water: 20%	default	800	Euler-Euler k−ε	
Kocherginsky N. et al. 2003 [20]	3D	oil, water	default	0.04 m/s	Oil: 1, 2.5, 5, 10%	default	1200	----	CFD & Experimental
Abdullah R. et al. 2013 [21]	2D	oil, water	atmosphere	0.04 m/s	---	default	130	VOF+RNG	Modelling 4 baffles locations
Huang S. 2005 [22]	2 D	oil, water	default	2 m3/h	Oil: 90% Water: 10%	default	---	Euler-Euler RSM	

Numerical simulations provide an efficient and economical method for studying multiphase flows; however, some problems and difficulties exist. Firstly, only half of the separator domain has been modeled because symmetrical fluid flow profiles are generally assumed [13,17-19,22]. This simplification may not be sufficiently realistic. Secondly, in some of the studies, the quality of the computational mesh system has not been validated [12-14,17-24]. Thirdly, extensive CFD research has been focused on separator internals such as baffles [13,16,21]. However, both simulations and experimental studies have shown that the internal structures play a minor role in improving the separation efficiency.

In this paper, an API separator was designed for an experimental study, and the effects of operating conditions on the oil / water separation process were analyzed. The whole computational domain is calculated with the same scale as the experimental setup. Both the CFD model and experimental method are used to investigate the oil / water separation process in a horizontal gravity separator.

Experimental Setup of A Gravity-Based Oil / Water Separator

The experimental investigations into the continuous separation of oil / water were performed in a flow loop, as illustrated in Fig. 1. Both oil and water were transferred from storage tanks to the test section with a pump made of 1-inch PVC pipe. Oil and water entered the test section from two pipes via a tee-junction. A flowmeter with a maximum capacity of 2.25 m^3/h was located on each of the flow lines (water and oil) to ensure the inlet oil velocity is the same as the water velocity. A pressure sensor was attached to the test section. After the pumps, each fluid had a bypass pipe to control the flow rate in the mainline. An inline pipe mixer with 12 blades was placed in the pipe to ensure adequate mixing for each experimental test. Fluids passed through the mixer had a homogeneous oil / water mixture with a average oil droplet diameter of approximately 200 μm. The fluid mixture then ran into the separator tank, where the oil and water separated. The separator tank had a length of 2.28 m (90 inches) and a width and height of 0.3556 m (14 inches).

Three baffles with different functions were placed in the separator. The first baffle called the flow spreading baffle was 0.127 m (5 inches) from the inlet wall and was used to reduce the inlet flow rate. The reduction of the inlet flow rate is essential because it is directly related to the oil rising time, which will further affect the separation efficiency. The space from the inlet wall to the first baffle is defined as Zone 1. The second baffle was located 1.778 m (70 inches) from the first baffle, with a height of 0.1778 m (7 inches). This baffle determines the oil-water main separation

range, defined as Zone 2. The third baffle was located 0.254 m (10 inches) from the end of the separator and was used to further separate the oil in order to re-cycle it back to the oil holding tank. The area between the third baffle and the end of the separator is defined as Zone 3. The 3D views of this separator are shown in Figs.2 and 3. The physical properties of the fluids and parameters are presented in Table 2.

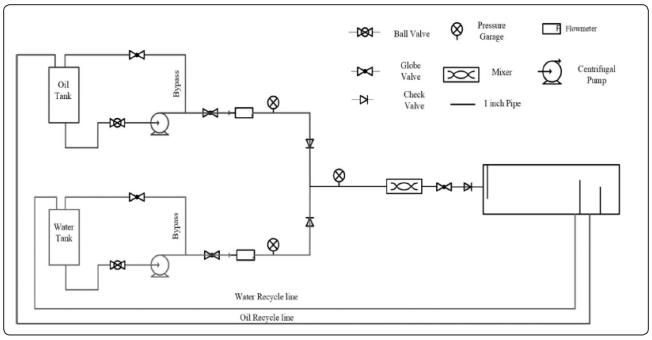

Figure 1: Schematic of the oil-water separation flow loop

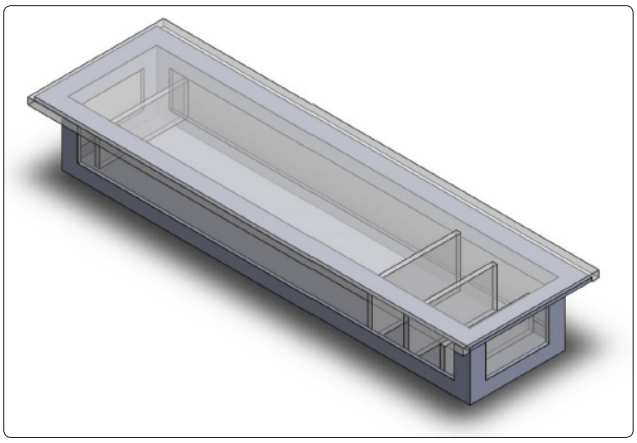

Figure 2: Isometric view of a 3-D geometric model of the designed separator

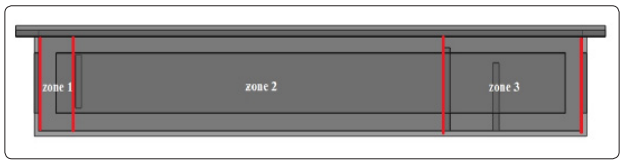

Figure 3: Front view of a 3-D geometric model of the oil / water separator

Table 2. Physical properties of fluids

Fluids properties	Value	Unit
Temperature	20	°C
Gravitational acceleration	9.81	m/s^2
Water density	992	kg/m^3
Oil density	872	kg/m^3
Dynamic viscosity of oil	0.0013	N/m2·s

The data acquisition system consists of two different frequency converters, National Instrument DAQ USB-6008, and NI 9211 Thermocouple Modules. The former is used to measure the flow rate, and the latter is used to measure the temperature. SignalExpress (National Instruments, 2015) and LabVIEW (National Instruments, 2015) programs are used for data acquisition.

Experimental Procedure and Method

To study the separation process, but to avoid the influence of these three layers changing over time, three sampling points were selected from the bottom of the water phase layer, and three more points were selected from the top of the oil phase layer. For each phase, the sampling points were evenly distributed in Zone 2 with the same horizontal position, as shown in Fig. 6. A maximum volume of 10 ml of samples was taken every minute. Time was measured with a stopwatch started from when the mixture entered Zone 2. The recording of residence time completed to an accuracy of approximately ± 0.5 min. The experiment began with a mixture phase in Zone 2, and the volume fraction of water was the same as the inlet value. As the residence time increased, oil droplets continuously moved to the top layer, and the water volume fraction in the bottom layer increased. The same phenomena happened to the oil volume fraction in the top layer. Separation efficiency is thus defined as the volume fraction of water in the bottom layer or the volume fraction of oil in the top layer.

$$\varepsilon = \frac{V_{water}}{V_{total}} \text{ or } \varepsilon = \frac{V_{oil}}{V_{total}} \quad (1)$$

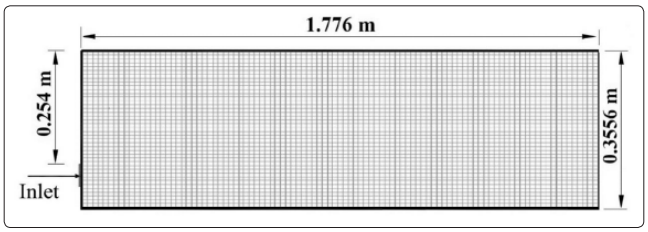

Figure 4: Schematic of the simulation domain

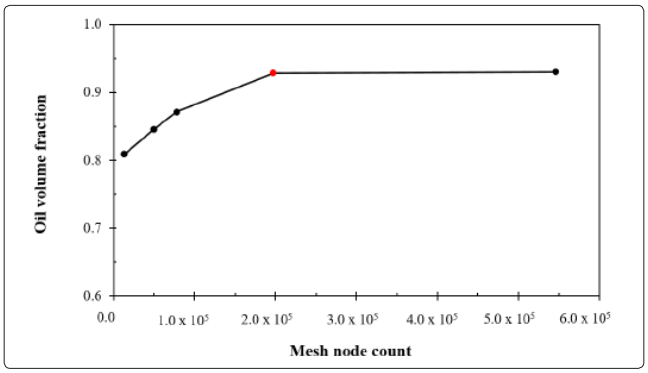

Figure 5: Mesh independence analysis

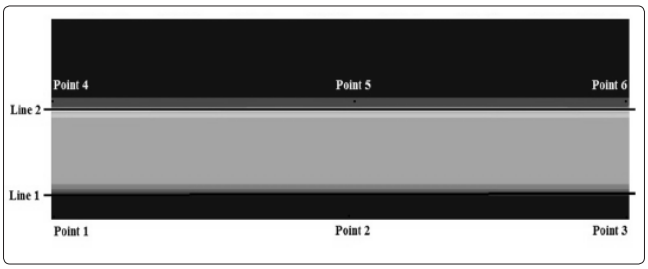

Figure 6: Sampling locations in Zone 2 (t = 900 s)

Numerical Simulation Method

The purpose of the CFD simulations was to obtain an oil / water separation process in the same operating conditions as in the experimental investigation so that results from the two could be compared. For this objective, a full-scale 2-D geometry as well as a mesh development for Zone 1 and Zone 2 is illustrated in Fig.

4. The inlet pipe had a 1-inch diameter. The entrance velocities were calculated by using the area of the entrance. The equation used to obtain the mixture inlet velocity was:

$$v_{inlet} = \frac{Q_{inlet}}{A_{pipe}} \quad (2)$$

where v_{inlet} is inlet velocity, Q_{inlet} is inlet volume flow rate, and A_{pipe} is cross area of the inlet pipe.

In the CFD model, the properties of the oil and water phase were the same as in the experimental study. The governing equations are the transient continuity and momentum equations, expressed as:

$$\frac{\partial}{\partial t}(\rho_m) + \nabla \cdot (\rho_m \vec{v}_m) = 0 \quad (3)$$

$$\frac{\partial}{\partial t}(\rho_m \overrightarrow{v_m}) + \nabla \cdot (\rho_m \overrightarrow{v_m} \overrightarrow{v_m})$$

$$= -\nabla p + \nabla \cdot [\mu_m (\nabla \overrightarrow{v_m} + \vec{v}_m^T)] + \rho_m \vec{g} + \vec{F} + \nabla \cdot \left(\sum_{k=1}^{n} \alpha_k \rho_k \vec{v}_{dr,k} \vec{v}_{dr,k} \right) \quad (4)$$

where v_m is velocity vector, F is body force, $v_{dr,k}$ is the drift velocity for secondary phase k, $v_{dr,k} = v_k - v_m$. Also, in Eq. (4), the mixture density p_m and mixture viscosity μ_m changes with the volume fraction of each phase; therefore, p_m is defined as

$\rho_m = \sum_{k=1}^{n} \alpha_k \rho_k$, and μ_m is defined as $\mu_m = \sum_{k=1}^{n} \alpha_k \mu_k$, where, α_k is the volume fraction of phase k, n is the number of phases.

The multiphase flow model used was the Volume of Fluid (VOF) with two Eulerian phases, in explicit time integration. For the viscous model, the laminar model was selected due to the laminar flow in Zone 2 of the experimental model. Gravitational acceleration was activated in the negative y-direction with the value of $9.81 m/s^2$. The transient process was defined with a total simulation time between 15 to 30 minutes for all cases. The time step value was chosen using the Courant-Friedrich criterion, which is one of the most common ways to check the stability of an explicit scheme. The simulation includes the filling process; therefore, in the initial condition for Zones 1 and 2 had no mixture. Standard initialization with the "Pressure Implicit with Splitting of Operator" (PISO) scheme for pressure-velocity coupling was chosen. The governing equations, together with the initial and boundary conditions, were solved in Fluent 16.2. Integrating the governing equation for each control-volume yielded discrete equations that conserve each quantity on a control-volume basis. The algebraic equations were solved iteratively. When the iterative cycle was satisfied, the calculation progressed through the remaining time steps.

The separator geometry and meshing were developed using ANSYS Fluent 16.2. A mesh independence study was conducted, and a very fine mesh was selected to achieve high accuracy. Different element sizes, shown in Table 3, were selected to create different discretizations on the separator. The oil volume fraction and the changes in the oil volume fraction predicted with different mesh sizes are presented in Table 3.

As presented in Fig. 5, an element size of 12.7×10^{-4} m, with a total quantity of 197,541 nodes, was selected for the simulations. In Table 3, the oil volume fraction refers to the maximum oil volume fraction in the oil phase. The minimum orthogonal quality of this mesh is 1.0; the average skewness is 0.0, and the average aspect ratio of the mesh is 1.414.

Table 3: Mesh independence study for separation efficiency

Element size (10^{-4} m)	Node number	Oil volume fraction	Change in oil volume fraction [%]
5.08	546,156	0.9301	-
12.7	197,541	0.9287	0.09
20.32	77,964	0.8714	1.46
25.4	49,771	0.8458	3.94
50.8	12,987	0.8091	5.90

Results and Discussions

Experimental Results

The separation efficiency is presented in terms of oil volume fraction in the water phase. The location of the sample is shown in Fig. 6. Zone 2 is vertically divided into three regimes; Regime 1 is the area located above Line 2, defined as the top layer, and is mainly occupied by the oil phase. Regime 2 is the area located below Line 1, which is defined as the bottom layer, with water as the main phase in this layer; Regime 3 is the area between Line 1 and Line 2, defined as the mixture layer. The vertical location of Line 1 and Line 2 changed during the filling process; however, the locations of Points 1 to 3 were fixed. Samples were taken every minute from these three points during the separation process, an average value for these three samples values were used for data analysis in the results section. The same sample locations are maintained in the experimental and numerical studies. Each operating condition was repeated at least twice.

Uncertainty Analysis

In the experimental study, several variables contribute to the overall uncertainty: the flow meter, the valves, the pressure sensor, and the analytical balance. Other operating uncertainties are assumed negligible, such as the change of environmental temperature during the experiments, noise around the lab, and other such factors. Therefore, according to the Kline and McClintock [27] uncertainty analysis method, the main equation to estimate the uncertainty of separation efficiency represented by oil concentration is

$$E = \frac{\sigma_R}{E_{C_{oil}}} = \sqrt{\frac{\delta W_{oil}{}^2}{W_{oil}} + \frac{\delta W_{total}{}^2}{W_{total}}} \quad (5)$$

Based on Eq. (5), the uncertainty for this experimental study was determined to be ±2.75%.

Effect of inlet velocity on the separation process

In this experimental study, the oil volume fractions in the water phase were measured each minute during the separation process. To better analyze the separation process, a non-dimensional time, t*, was defined as follows:

$$t^* = \frac{v \cdot t}{d_o{}^2} \quad (6)$$

where, v is the kinematic viscosity of water, d_o is the oil droplet diameter, and t is the resident time. Preliminary experiments showed that oil / water separation took place immediately when the mixture ran into Zone 2, and two separate transparent phases started to form. The initial oil volume fraction in the water phase reduced by approximately 70 % in the first two minutes. Measurements of the water volume fraction in the oil phase also demonstrated that separation takes place immediately when $t^* < 500$. Similarly, but even better, the separation was observed with the decrease of the inlet flow rate, as shown in Figs. 7 and

8. More attention should be given to the separation process when t* < 500. The separation efficiency reaches 95% in all operating conditions when t* > 1000. Increasing the inlet flow rate, has a negative effect on the oil / water separation process, as shown in Fig.7. The oil volume fraction slightly changed in the range 500 < t* < 1000 when the inlet velocity was 2.5 GPM. One possible reason for this phenomenon is that an increase in the inlet velocity will increase the fluid turbulence in the separator, which results in the oil droplets having relatively higher horizontal velocity. The determining factor to separate oil droplets from the water phase is the residence time. A high horizontal velocity will reduce residence time, which means that the oil droplets have less time to rise from the water phase. Therefore, separation efficiency is reduced.

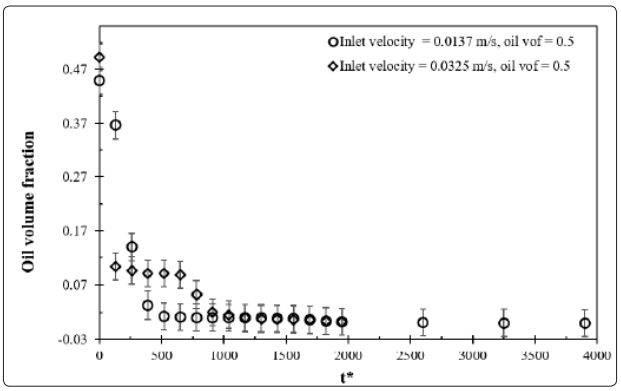

Figure 7: The effect of inlet velocity on separation efficiency

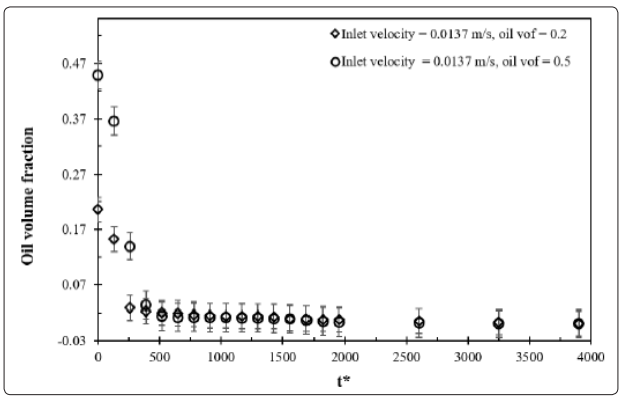

Figure 8: The effect of oil volume fraction on separation efficiency

Effect of the oil volume fraction on the separation process

The differences in the level of the oil volume fraction affect the separation process in the first several minutes. For an initial oil volume fraction of 0.5, Fig. 8 shows an increase in the initial oil volume fraction from 0.2 to 0.5, which slightly decreased the changes of the oil volume fraction in the water phase in the range t* < 500, from 90 % to 75 %. This tendency is attributed to the increase in the total number of oil droplets. A relatively large number of oil droplets increases the frequency of droplet collisions, which is degrading the oil droplet coalescence efficiency [28]. Another possible reason is the increase in the viscosity of the multiphase flow. However, the total separation time is not affected by the oil volume fraction. The reason is that increasing the oil volume fraction only changes the oil droplet concentration in the water phase; it does not affect the resident time. Therefore, it has a negligible effect on the total time of separation.

The experimental results for oil droplets in a water system are for an oil volume fraction of less than 0.5. In contrast, water droplets in an oil phase are defined as a system with a water volume fraction of less than 0.5 [19]. Water in an oil system is only investigated with the CFD simulations.

Simulation Results

In this section, the oil / water separation process is studied numerically, while the oil volume fraction contour and the velocity vector are presented to understand the separation process better. Also, with the same operating conditions, the results of the numerical prediction are compared with the experimental results to validate the simulation model.

Validation of the CFD Model

The oil volume fractions in the water samples for both the experimental study and the simulation study are presented to compare the results. Experimental data points were taken every minute. The oil volume fraction curve obtained from the numerical simulation model shows a dramatic drop in the oil volume fraction at the very beginning (t* < 200) of operation. The oil volume fraction decreases very slightly when t* ranges from 650 to 2000 until all the oil droplets were separated from the water phase.

In this study, two numerical operating conditions with different oil volume fractions were investigated to further validate the numerical model. As shown in Figs. 9 and 10, both numerical predictions had good agreement with experimental results. This agreement suggests the numerical model setting is suitable, and the numerical predictions are accurate for the other simulation cases in this paper. The fundamental operating condition case is selected as an oil volume fraction of 0.2, the operating temperature is 20 °C, and the inlet flow velocity is 0.0137 *m/s*.

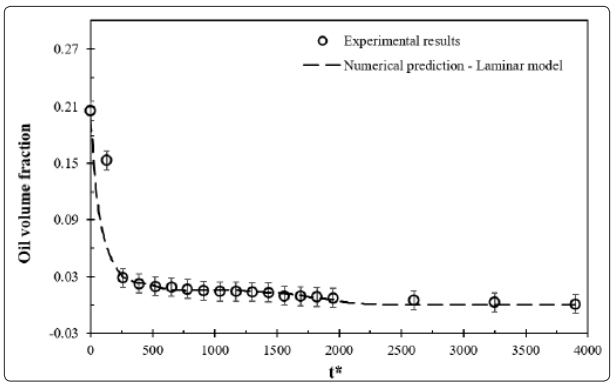

Figure 9: Validation of numerical results: inlet velocity = 0.0137 m/s, ε_{oil} = 0.2, T = 20°*C*

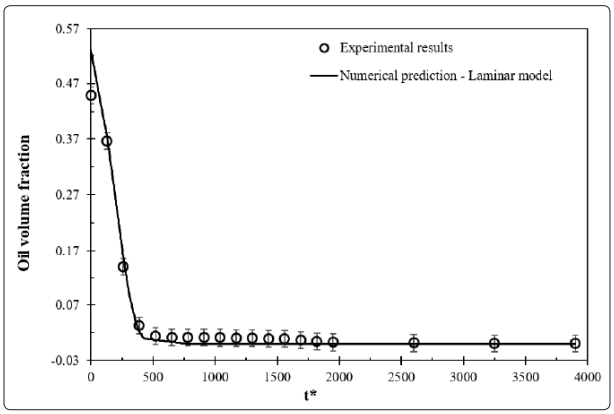

Figure 10: Validation of numerical results: inlet velocity = 0.0137 m/s, ε_{oil} = 0.5, T = 20 °*C*

Contours of oil volume fraction and velocity vector fields

The oil volume fraction in the water phase is presented in this

section. Because the top area of the separator has no oil or water phases, thus, the oil volume fraction is zero. Contours of the oil volume fraction in the separator Zone 2 at 300, 600, and 900 s are shown in Fig. 11. There is a regime where the separated oil phase moved firmly upward with time, and the thickness of the separated phase increases with time, as presented in Fig. 11. The maximum oil volume fraction in the oil phase was 0.98. As the separation process starts and continues, the water volume fraction in the bottom layer increases as the oil volume fraction decreases with time. In the top layer, the oil volume fraction increases while the water volume fraction decreased. Thus, the separated water phase and oil phases formed in the separator. Also, the oil volume fraction distribution results show that there was a mixed zone at the entrance where the oil volume fraction is relatively low compared to the same vertical location of the rest of the separator. This is because the oil volume fraction of the mixture is 0.2, which is lower than the volume in the separated phase. When the mixture mixes with the separated oil phase at the entrance, it results in the divergence of the oil volume fraction in that area.

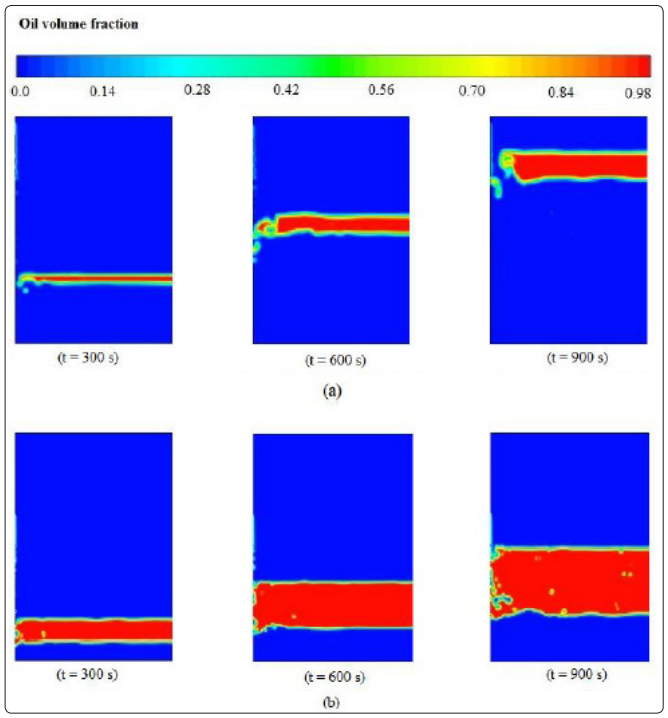

Figure 11: Contours of oil volume fraction: (a) Initial oil volume fraction = 0.2, (b) Initial oil volume fraction = 0.5

The fluid velocity vectors in Zone 1 are shown in Fig. 12. Evaluation of mixing properties of different times has been restricted to visual observation of the velocity profiles. Due to the large size of Zone 2, in order to obtain a clear and detailed velocity vector, only 1/8 length of Zone 2 was selected to present the contours. The fluid was dispersed at the bottom of the separator, where oil droplets start to rise because of the buoyancy effect. The general flow patterns for the configurations presented show high velocities at the inlet. At t = 300 s, as the flow reaches the bottom, the velocity drops significantly. In Zone 2, oil droplets move with constant velocity, which follows Stokes' law.

As the filling process continued, at t = 600 s, the fluid level inside the tank increased; therefore, there is a small mixing zone near the inlet due to high relative velocity. The velocity dropped back to the terminal velocity after the mixing zone. The mixing zone area became more significant when the fluid level was close to the same vertical height as the vertical location of the inlet pipe, as shown when t = 900 s in Fig. 11. Also, a very small vortex zone is created when t = 900 s. Behin and Bahrami [19] observed a similar fluid behavior in their study with a horizontal separator. Mixing zone, plug zone, and dead zone were defined according to the velocity vector in their study. Their results also suggested that an increase in the inlet flow rate leads to an increase in mixing zone volume. However, the main objective is to estimate the trends of the flow behavior in the Behin and Bahrami study [19], such as the percentage of mixing zone volume and dead zone volume.

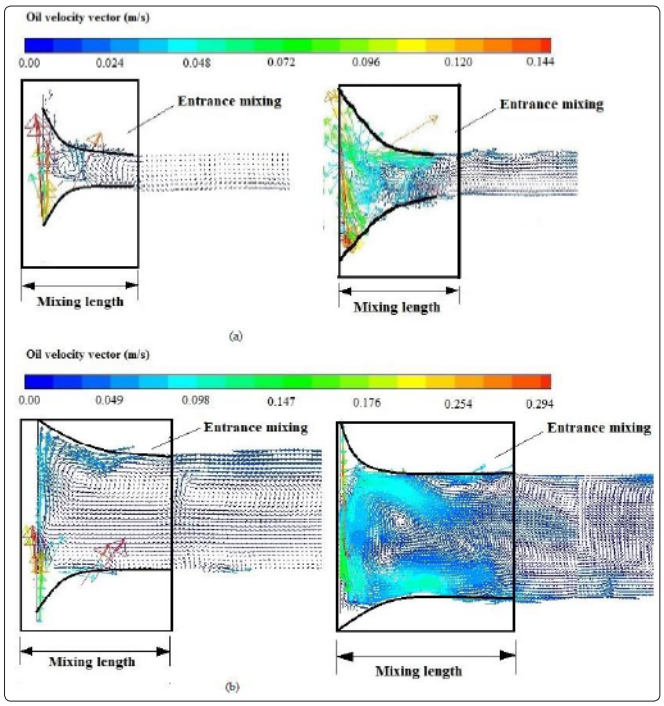

Figure 12: Velocity vectors: (a) Initial oil volume fraction = 0.2 (b) Initial oil volume fraction = 0.5.

Effect of velocity on the mixing length

There was a mixing zone formed at the entrance of the inlet, as shown in Fig. 11. The mixing length depended on the inlet velocity. Therefore, the velocity effect on the mixing length is investigated in this section. The velocity simulation cases are listed in Table 4. The Reynolds number of fluids in the separator plays a prominent role in determining the fluid's behavior. Also, since the simulation model of this study is the mixture entering into a separator, therefore, it is a category to open channel flow. The Reynolds number in the open channel is

$$Re = \rho l v_{oc}/\mu \qquad (7)$$

where v_{oc} is the fluid velocity in the separator, and l is the characteristic length. The characteristic length for this geometry is

$$l = A/P = l_h y/(2y + l_h) \qquad (8)$$

where l_h is the length of the separator, y is the height of fluid in the separator, $y = Q_{in}/A_s$, which is a function of the inlet flow rate. Therefore, the equation for Renumber in this open channel is

$$Re = \frac{\rho}{\mu} \cdot \frac{A_p^2 \cdot v_{in}^2}{(l_h^2 + 2A_p v_{in})} \qquad (9)$$

When the inlet velocity was less than 0.1 m/s is Regime 1, who is identified as linear laminar flow zone since the Reynolds number of

the fluid in the separator is Re < 5 [29] [30]; Regime 2 is when the inlet velocity was between 0.1 and 0.5 m/s. Regime 2 is identified as non-linear laminar flow since the Reynolds number in this zone is between 5 < Re < 100 [30]; Regime 3 is when the inlet velocity was higher than 1.0 m/s. In Regime 3, the Reynolds number is 500 < Re < 1000, thus, Regime 3 is identified as transition flow. The data are taken from Line 2 in Fig. 6. The mixing length was determined by the average horizontal length over different times when oil volume is one.

The results and comparison of the inlet velocity in the entrance pipe effect on mixing length are presented in Table 4. Increasing the inlet velocity increased the mixing length. In linear laminar flow [29] [30], the fluid movement is dominated by viscous forces. Therefore, the inlet velocity has a negligible effect on the mixing length (l_m/L <5 %), as shown in Table 4. In non-linear laminar flow, where the fluid velocity is in Regime 2, the flow in the separator was still in the laminar regime. However, the impact of inlet velocity on the chaos of fluid at the entrance becomes significant at this Re range. The mixing length increases with the increase of inlet velocity in Regime 2, as presented in Table 4. In Regime 3, the fluid in the separator was in the transition range, which means that the viscous forces no longer dominate the fluid movement. Fluid moves chaotically at the entrance. As shown in Table 4, the mixing length increases sharply from Regime 1 to Regime 3. The main reason is that oil droplets increase inlet velocity as the droplet's horizontal velocity increases. In the same separation time, oil droplets move further. This causes a longer mixing length.

Table 4: Impact of inlet velocity on mixing length

Regime	Cases	Velocity (m/s)	Mixing length *lm* (m)	Percentage *lm*/ *L*(%)
Regime 1 (linear laminar flow)	Case # 1	0.0137	0.028	1.57
	Case # 2	0.0274	0.081	4.57
Regime 2 (non-linear laminar flow)	Case # 3	0.105	0.555	31.2
	Case # 4	0.274	0.639	35.9
Regime 3 (transition flow)	Case # 5	1.05	1.40	78.8
	Case # 6	1.5	1.42	79.9
	Case # 7	1.75	1.56	87.7

Conclusions

In this paper, experiments and numerical simulations were utilized to investigate phase separation with entrance mixing. The effects of inlet flow rate and oil volume fraction on the oil / water separation process were studied experimentally. The results of the experiments show that the inlet flow rate has a negative effect on the oil / water separation process. Increasing the initial oil volume fraction increases the oil volume fraction in the water phase in the range t* < 500, but it does not affect the total separation time.

Oil volume fractions and the velocity vector distribution in the separator were investigated with numerical techniques. Both of the results showed that there was a mixing zone located at the entrance, which had a lower oil volume fraction and a higher velocity than downstream in the separator. Additionally, this paper showed that the mixing length was closely related to the inlet velocity from the entrance pipe. When the fluid in the separator was in the laminar regime, the mixing length is less than 40 % of the total separator length; however, increasing the inlet velocity until the fluid in the separator was in the transient regime, resulted in the mixing length occupying 90 % of the total separator length.

Acknowledgments

The authors thank the financial support from the Natural Sciences and Engineering Research Council of Canada (NSERC) and the NL Innovation Council.

Abbreviations

2-D: Two dimensional
3-D: Three dimensional
API: American Petroleum Institute
CFD: Computational fluid dynamics
DAQ: Data acquisition system
GPM: Gallon per minute
VOF: Volume of fluid

References

1. Friberg S, Larsson K, Sjöblom J, eds, (2003) Food Emulsions CRC Press.
2. Sjöblom J, Aske N, Auflem IH, Brandal Ø, Havre TE, et al. (2003) Our Current Understanding of Water-in-Crude Oil Emulsions. Recent Characterization Techniques and High Pressure Performance. Adv Colloid Interface Sci 102: 399-473.
3. Schwarzkopf JD, Sommerfeld M, Crowe CT, Tsuji Y (2011) Multiphase Flows with Droplets and Particles, CRC press.
4. Hinze JO (1955) Fundamentals of the Hydrodynamic Mechanism of Splitting in Dispersion Processes. AIChE J 1: 289-295.
5. Arnold K, Stewart M, (1999) Surface Production Operations, Volume 2: Design of Gas- Handling Systems and Facilities, Elsevier.
6. Rowley ME, Davies G (1988) Design of Plate Separators for the Separation of Oil- Water Dispersions. Chem Eng Res Des 66: 313-322.
7. Aymong GG (1988) Oil-Water Separator.
8. Zhenlin L, Shouping D, Jian Z (1999) Internal Flow Field in Gravity Oil-Gas-Water Separators. CHINA Pet 27: 10-12.
9. Schlieper L, Chatterjee M, Henschke M, Pfennig A (2004) Liquid–Liquid Phase Separation in Gravity Settler with Inclined Plates. AIChE J 50: 802-811.
10. Colenbrander GW (1991) CFD in Research for the Petrochemical Industry. Appl Sci Res 48: 211-245.
11. Foumeny EA, Benyahia F (1993) Can CFD Improve the Handling of Air, Gas and Gas-Liquid Mixtures? Chem Eng Prog 89: 21-26.
12. Lee JM, Khan R, Phelps D (2008) Debottlenecking and CFD Studies of High-and Low-Pressure Production Separators. SPE Annual Technical Conference and Exhibition Society of Petroleum Engineers.
13. Lu Y, Lee JM, Phelps D, Chase R (2007) Effect of Internal Baffles on Volumetric Utilization of an FWKO--A CFD Evaluation. SPE Annual Technical Conference and Exhibition, Society of Petroleum Engineers.
14. Lee C-M, van Dijk E, Legg M, Byeseda J (2004) Field Confirmation of CFD Design for FPSO-Mounted Separator. Offshore Technology Conference Offshore Technology Conference.
15. Austrheim T (2006) Experimental Characterization of High-Pressure Natural Gas Scrubbers.
16. Pourahmadi Laleh (2010) CFD Simulation of Multiphase Separators.
17. Liang Y, Zhao S, Jiang X, Jia X, Li W (2013) Numerical Simulation on Flow Field of Oilfield Three-Phase Separator. J Appl Math.

18. Zhang X, Cheng Y, Nie S, Ji H, Liu L (2013) Simulation of Multiphase Flow of the Oil-Water Separation in a Rotating Packed Bed for Oil Purification. Math Probl Eng.
19. Behin J, Bahrami S (2012) Modeling an Industrial Dissolved Air Flotation Tank Used for eparating Oil from Wastewater. Chem Eng Process Process Intensif 59: 1-8.
20. Kocherginsky NM, Tan CL, Lu WF (2003) Demulsification of Water-in-Oil Emulsions via Filtration through a Hydrophilic Polymer Membrane. J Memb Sci 2: 117-128.
21. Hussein HA, Abdullah R, Harun S, Abdulkhaleq M (2013) Numerical Model of Baffle Location Effect on Flow Pattern in Oil and Water Gravity Separator Tanks. World Appl Sci J 26: 1351-1356.
22. Huang S (2005) Numerical Simulation of Oil-water Hydrocyclone Using Reynolds-Stress Model for Eulerian Multiphase Flows. Can J Chem Eng 83: 829-834.
23. Yuling L, Limin H, Guodong W (2008) Numerical Simulation of Flow Field inside Gravitational Separator with Different Internals. China Pet Mach 36: 12-16.
24. Jayanti S, Hewitt GF (1991) Review of Literature on Dispersed Two-Phase Flow with a View to CFD Modeling. AEA Technol Report AEA-APS-0099.
25. Luo HB, Feng J, Yang Q, ZHANG X, SHU H (2007) CFD Simulation of the Inner Flow Fie1d of the Gas-Liquid Measure Cyclones. Mech Eng 1: 74-76.
26. Noroozi S, Hashemabadi SH (2009) CFD Simulation of Inlet Design Effect on Deoiling Hydrocyclone Separation Efficiency. Chem Eng Technol Ind Chem Equipment-Process Eng 32: 1885-1893.
27. Kline SJ, McClintock FA (1953) Describing Uncertainties in Single-Sample Experiments. Mech Eng 75: 3-8.
28. Mohammadi M, Shahhosseini S, Bayat M (2012) Direct Numerical Simulation of Water Droplet Coalescence in the Oil. Int J Heat Fluid Flow 36: 58-71.
29. Robinson SK (1990) A Review of Vortex Structures and Associated Coherent Motions in Turbulent Boundary Layers. Structure of Turbulence and Drag Reduction Springer 23-50.
30. Bear J (1972) Dynamics of Fluids in Porous Materials. Elsevier New York 3: 125- 127.